Karger
OPEN ACCESS

Medical Principles and Practice

Med Princ Pract , DOI: 10.1159/000552577

Received: December 19, 2025

Accepted: May 14, 2026

Published online: May 22, 2026

Histopathological Analysis of Adipose-Derived Mesenchymal Stem Cells and Their Osteogenic Derivatives in Promoting Bone Regeneration in Model of Fracture Non-Union

Maslennikov S, Danukalo M, Isachenko M, Avramenko Y, Holovakha M, Kolesnyk Y

ISSN: 1011-7571 (Print), eISSN: 1423-0151 (Online)

https://www.karger.com/MPP

Medical Principles and Practice

Abstract

Objective. To perform a histopathological analysis of the effects of mesenchymal stem cells (MSCs) and their osteogenically differentiated derivatives (Dif-MSCs) on reparative processes in bone tissue using an experimental model of fracture nonunion. ***Subjects and Methods***. Fifteen male rabbits aged 3 months were randomly assigned to three groups: control with induced femoral nonunion (n=5), nonunion treated with adipose-derived MSCs (n=5), and nonunion treated with Dif-MSCs (n=5). MSCs were isolated from lipoaspirate, cultured to passage 3, and differentiated osteogenically for 4 weeks. A 5-mm bone defect was created surgically, and cells were injected into the defect zone on day 7. Animals were euthanized at 6 weeks post-injection. Bone specimens underwent fixation, decalcification, histological staining (hematoxylin-eosin and Van Gieson), and quantitative analysis of osteoblasts and osteocytes using ImageJ. Statistical analysis included one-way ANOVA and Welch's t-test. ***Results***. Macroscopic and histological evaluation revealed a gradation in regeneration: control group showed predominant fibrous tissue with immature bone and inflammation; MSCs group exhibited fibrocartilaginous callus with immature bone, bone marrow formation, and increased osteoblasts (52.0 ± 16.2 per 10 HPF vs. control 28.6 ± 7.0, $p = 0.032$); Dif-MSCs group demonstrated mature lamellar bone, organized osteons, mature bone marrow, and higher osteocytes (vs. MSCs, $p = 0.006$). ANOVA indicated trends in osteoblast increases ($p = 0.092$) and significant osteocyte variability ($p = 0.014$). ***Conclusion***. Undifferentiated MSCs enhance early osteogenesis via endochondral ossification, while Dif-MSCs promote advanced maturation through mixed intramembranous and endochondral pathways, suggesting superior efficacy for treating fracture nonunion.

Introduction

Nonunion of long bone fractures occurs relatively infrequently, it remains one of the most challenging complications in orthopedics and traumatology. Delayed union, defined as the absence of bone consolidation within three months [1], affects approximately 600,000 fracture cases annually worldwide. Despite limited international statistical data, the prevalence of nonunion is estimated to range from 5% to 10%, depending on fracture location [2]. Nonunion causes substantial functional impairment and frequently requires repeated surgical interventions, markedly increasing the socioeconomic burden on society. In the context of active hostilities, bone injury healing remains a particularly pressing issue. Approximately 90% of combat-related injuries involve the extremities, one-third of which are fractures of long tubular bones. Due to their severity, most of these injuries result in amputations, with a considerable proportion complicated by delayed union or nonunion [3].

Effective management of these complications relies on growth factor delivery, osteoconductive scaffolds, cellular technologies at the fracture site, and adequate mechanical stabilization of the biological environment – an approach known as the “diamond concept” [4]. In this context, cellular therapies, particularly the use of mesenchymal stem cells (MSCs), have demonstrated high efficacy due to their capacity for self-renewal, differentiation, and secretion of biologically active factors that regulate the regeneration of damaged tissues [5]. Adipose tissue is considered an attractive alternative to bone marrow as a source of MSCs, as it is more readily accessible, contains a higher yield of stem cells, and is largely free of ethical concerns [6, 7]. Some investigators suggest that the osteogenic potential of adipose-derived stem cells (ADSCs) may exceed that of bone marrow-derived cells [8], although these findings require further validation. Given these advantages, the osteogenic differentiation capacity of MSCs remains a key research focus in traumatology for managing traumatic delayed union or nonunion.

Osteogenic differentiation of MSCs for bone repair is a well-established field. Bone marrow-derived MSCs (BM-MSCs) have been extensively studied for their superior osteogenic potential compared with ADSCs, which, despite

easier procurement and higher yield, typically exhibit reduced osteogenic capacity [9]. Numerous studies have compared undifferentiated MSCs with their osteogenically differentiated counterparts in bone regeneration models. For example, in a rat cranial defect model, BM-MSCs induced faster and more substantial bone formation than ADSCs [10]. In addition, an in vivo study using a shape memory polymer scaffold demonstrated that differentiated umbilical cord MSCs substantially enhanced new bone formation compared with undifferentiated cells, underscoring the advantages of pre-differentiation [11]. However, *in vitro* and *in vivo* comparisons reveal notable inconsistencies. While undifferentiated MSCs may promote osteogenesis through paracrine factors such as osteoprotegerin, *in vivo* studies generally demonstrate superior direct bone formation with differentiated MSCs [12]. In a canine radial fracture model, sheets of osteogenically differentiated MSCs outperformed their undifferentiated counterparts in facilitating recovery, suggesting that pre-differentiation can accelerate the healing process [13]. Conversely, some studies, including those in guinea pig fracture models, found no significant differences in outcomes between differentiated and undifferentiated MSCs, although both outperformed the controls [14]. These findings emphasize that results are strongly influenced by cell origin, differentiation status, and experimental conditions [15].

Despite extensive investigation, the impact of pre-differentiation on the mechanisms of tissue regeneration remains insufficiently understood [16]. It remains unclear whether undifferentiated MSCs, acting mainly through paracrine signaling and immunomodulation, or pre-differentiated cells, which directly contribute to matrix deposition, provide superior outcomes in clinical bone repair scenarios. Remaining gaps include the lack of direct comparative analyses in trauma-relevant models that evaluate long-term integration, as well as limited understanding of how differentiation state affects cellular survival and engraftment in hostile injury environments. The present study addresses these gaps by providing a comparative analysis of the regenerative process following the application of MSCs cultures and their osteogenically differentiated derivatives.

The aim of this study was to perform a histopathological analysis of the effects of mesenchymal stem cells and their osteogenically differentiated derivatives on reparative processes in bone tissue using an experimental model of fracture nonunion.

Materials and Methods

Animals and Study Design

The study included male rabbits (n = 15) aged 3 months, with a mean body weight of 2.94 ± 0.10 kg. The animals were randomly assigned to three groups. Group 1 consisted of control rabbits with an experimentally induced fracture nonunion. Group 2 included rabbits with fracture nonunion that received mesenchymal stem cells (MSCs) administered into the defect zone. Group 3 comprised rabbits with fracture nonunion treated by the implantation of MSCs that had undergone osteogenic differentiation (Dif-MSCs) into the fracture site. The sample size of n=5 animals per group was selected based on ethical considerations in accordance with the 3R principles (Replacement, Reduction, Refinement) outlined in the *International Guiding Principles for Biomedical Research Involving Animals* (CIOMS, 1985) and the *Guide for the Care and Use of Laboratory Animals* (National Research Council, 2011). This approach aimed to minimize the number of animals used while allowing for preliminary histopathological evaluation and statistical comparisons in this exploratory study. The experimental study involving laboratory animals was conducted in accordance with mentioned international ethical standards. The study protocol was reviewed and approved by the local bioethics committee (protocol No. 15, dated December 10, 2025). All stages of the study were carried out in a specially equipped *Cell Culture and Bioengineering Laboratory* (Certificate of Technical Competence of the Ministry of Health of Ukraine No. 181/23, dated December 21, 2023). The experiments were performed in compliance with high standards of equipment quality, aseptic conditions, sterility, and biological safety.

Isolation and Culture of Adipose-Derived Mesenchymal Stem Cells

A primary mesenchymal stem cell line was established from three donor rabbits included in the present study. Adipose tissue was harvested by the research team from subcutaneous (inguinal) and visceral (perirenal and gonadal) depots. Adipose-derived MSCs were isolated by enzymatic digestion with type I collagenase (SCR103, Sigma-Aldrich, USA) [17] and subsequently cultured under standard *in vitro* conditions. For the experiments, cells at passage 3 were used and divided into two groups. MSCs were cultured for 30 days in standard DMEM culture medium. For osteogenic differentiation, cells were induced for 4 weeks in a specialized osteogenic medium

consisting of low-glucose DMEM supplemented with pyruvate (lacking glutamine and phenol red), L-ascorbic acid (50 µg/mL), dexamethasone (10 nM), and β-glycerophosphate (10 mM). The 4-week induction period was selected to achieve full osteogenic differentiation, as opposed to pre-differentiation (e.g., 1-2 weeks). Differentiation was validated by a 3.8-fold increase in ALP activity (spectrophotometric assay at 405 nm, $p < 0.001$ vs. undifferentiated MSCs) and positive Alizarin Red S staining, with quantified calcium deposition covering 48.6% ± 9.2% of the culture area (image analysis via ImageJ, $p < 0.001$ vs. 1.8% ± 0.4% in undifferentiated controls). No spontaneous differentiation was observed in undifferentiated MSCs, confirming distinct cell states prior to implantation.

Surgical Procedure and Cell Delivery

The animals underwent surgery to establish an experimental model of femoral fracture nonunion. The femur was chosen as the target bone based on its anatomical suitability and the objectives of this stage. All procedures were performed under the principles of humane animal treatment. Premedication consisted of *meloxicam* (0.5 mg/kg IM) 30 min before surgery, followed 15 min later by *medetomidine* (*Medison*, 0.25 mg/kg IP). Anesthesia was induced with *Telazol* (10 mg/kg IM) and maintained with *isoflurane* (1-3% in 100% oxygen) via a tight-fitting face mask, with continuous monitoring of vital parameters. A linear incision was made over the middle third of the femur, followed by blunt muscle dissection and meticulous hemostasis. An angular-stable plate was applied and fixed with four cortical screws. A 5-mm bone defect was created between two adjacent screws using a surgical drill. The wound was irrigated with antiseptic solutions and closed in layers. An aseptic dressing was applied, and the limb was immobilized in an extended position with an elastic bandage for the first 5 postoperative days solely to prevent self-inflicted damage. No further immobilization was applied after day 5. From day 6 post-surgery, all animals were allowed full weight-bearing and unrestricted movement in their individual cages to simulate natural loading on the limb. Daily veterinary assessments confirmed no wound complications (infection, dehiscence, or inflammation) in any animal across all groups. All rabbits exhibited comparable full weight-bearing and normal cage activity from day 6 until the end of the study (6 weeks post-cell injection). This uniform postoperative protocol ensured standardization of mechanical stimulation and recovery conditions across the control, MSCs, and Dif-MSCs groups. Following the induction of sedation, on day 7 after creation of the bone defect, the rabbits received cell injections suspended in culture medium (1.2×10^7 cells/ml in 1 ml culture medium) directly into the defect zone (percutaneous delivery route) under C-arm fluoroscopic guidance. The experimental timeline was as follows: Day 0 – surgical creation of bone defect; Day 7 – cell injection; Week 6 post-injection (Week 7 post-defect) – euthanasia and sample collection following radiographic confirmation of union status.

Histological Processing and Analysis

The bone tissue was initially fixed in a 4% buffered formalin solution. After fixation, the specimens were carefully cleared of surrounding soft tissues, sectioned into fragments approximately 1 × 1 cm in size, and rinsed under running water for 2 hours. Decalcification was performed over a period of 15 days in a 20% buffered EDTA solution (ethylenediaminetetraacetic acid, pH 7.0–7.5). The endpoint of decalcification was determined using a mobile X-ray system (X-MIND UNITY, Acteon Group, France) (Fig. 1).

Pathohistological processing was performed using a classical protocol with dehydration in ascending concentrations of ethanol, followed by specimen clearing in a chloroform-based mixture. Staining was carried out using hematoxylin-eosin (H&E) and Van Gieson methods. Photomicrographs were analyzed using the open-source software ImageJ (National Institutes of Health, USA). Cells were identified morphologically using standard histological criteria without immunostaining: osteoblasts as cuboidal cells with hyperchromatic nuclei along bone surfaces and osteocytes as embedded cells in lacunae within the bone matrix. Counts were performed manually in a blinded manner across 10 high-power fields (HPF, ×400) per section, with at least three sections per animal (totaling 30 HPF per sample). Cell numbers were expressed as absolute counts per 10 HPF and averaged across sections. Quantitative analysis of osteoblasts and osteocytes was performed exclusively in the callus regeneration zone of specimens obtained 6 weeks after cell injection.

Radiographic examinations

Subsequent radiographic examinations were performed at weeks 3 and 7 after cell administration using standard parameters (tissue thickness 2-4 cm, tube voltage 50-52 kV, tube current-exposure time product 0.6-1.3 mAs). Animals were positioned supine with the operated limb abducted and internally rotated by three-quarters.

Primary outcome measures were the percentage of bridging callus (% Bridging Callus), a quantitative indicator of callus formation during secondary fracture healing, and the cortical thickness index (CTI) for non-invasive dynamic monitoring of bone mineral density. The CTI also served as a marker for the absence of systemic bone pathology (e.g., osteoporosis) and the condition of bone tissue in the fracture zone [18].

Statistical analysis

Statistical analysis was performed using one-way analysis of variance (ANOVA) in the Statistica software package (license No. JPZ804I382130ARCN10-J). Continuous variables are presented as the median (Q1 and Q3). All parameters were compared using one-way ANOVA, followed – when statistical significance was detected – by Tukey's post hoc test for multiple comparisons. A two-sided p value of < 0.05 was considered statistically significant for all analyses. In addition, Welch's t-test was applied for pairwise comparisons between groups.

Results

After induction of osteogenic differentiation, only small, scattered calcium deposits – possibly artifactual or baseline in nature – were observed in the control MSCs on day 8. In contrast, Alizarin Red staining in the osteogenic medium was markedly more extensive and diffuse, covering a substantially greater area and likely representing an early stage of mineralized extracellular matrix formation (Fig. 2).

Macroscopic examination of bone specimens from both groups revealed preservation of the femur's typical linear diaphyseal configuration, characterized by a cylindrical shape and slight sagittal curvature. The fracture site was no longer discernible, with intact bone continuity confirming complete fracture consolidation. A spindle-shaped periosteal thickening was observed beneath the fixation device at the former fracture site, consistent with secondary healing due to fixation instability and the lack of rigid contact between bone fragments. Fixator positions remained unchanged in all cases, although isolated screw loosening and migration occurred. In the MSCs-treated group, the fixation plate was partially integrated into the regenerating tissues, surrounded by a pronounced fibrous capsule around the plate and modeled fracture area. In contrast, Dif-MSCs specimens demonstrated a higher degree of tissue ossification, evidenced by osteophyte formation around the plate and screws as well as ossification foci within the surrounding fibrous tissue.

Histological specimens from the MSCs group showed soft fibrous connective tissue with initial signs of consolidation in the defect area. The bone defect was not fully bridged by mature bone tissue, indicating predominant fibrous formation or insufficient osteogenesis without additional stimulation. In contrast, the Dif-MSCs group exhibited denser and more compact tissue filling the defect, with newly formed tissue that more closely resembled mature or transitional (cartilaginous) bone in both color and texture. These findings indicate a superior osteoinductive effect of the applied therapy.

Microscopic analysis of the control group showed that the defect was predominantly filled with fibrous tissue containing immature bony spicules and trabeculae, more developed and anastomosing at the periphery (Fig. 3a, b). The reparative tissue was heterogeneous, with small residual cartilaginous foci, focal mild inflammation, increased vascularity and edema, but without bone marrow formation or signs of remodeling (Fig. 3c, d). Osteoblasts averaged 28.6 ± 7.0 per 10 HPF, and osteocytes 58.4 ± 12.0 per 10 HPF (Fig. 3c).

In the MSCs group, a well-formed fibrocartilaginous callus predominated with immature coarse-fibered bone, calcified cartilaginous spicules and active remodeling (Fig. 4a, b, c). Central bone marrow formation and numerous resorption canals were evident (Fig. 4d, e). No inflammation was observed. Hypertrophic chondrocytes showed degenerative and apoptotic changes (Fig. 4f). Osteoblasts averaged 52.0 ± 16.2 per 10 HPF, osteocytes 45.3 ± 5.62 per 10 HPF, and small numbers of osteoclasts were present at sites of mineralized cartilage (Fig. 4f).

In the Dif-MSCs group, the defect was predominantly filled with mature cancellous and compact bone containing organized lamellar structures and primary osteons (Fig. 5a, d). Mature tri-lineage red bone marrow occupied the intertrabecular spaces (Fig. 5b). Minimal residual fibrous tissue was present only at the defect margins (Fig. 5c). The cartilaginous callus was almost completely replaced by bone, with only isolated residual foci remaining. Osteoblasts averaged 42.7 ± 11.5 per 10 HPF, and osteocytes 65.7 ± 9.76 per 10 HPF (Fig. 5d, e).

One-way analysis of variance (ANOVA) for osteoblast counts yielded an F-value of 3.064 with a p value of 0.092, indicating no statistically significant overall differences between the groups at the $\alpha = 0.05$ level, although a trend

toward increased values in the experimental groups was evident “Table 1”. Pairwise comparisons using Welch’s t-test showed a statistically significant difference in osteoblast numbers between the control and MSCs groups (p = 0.032), indicating that undifferentiated cells substantially enhance cellular proliferation and early osteogenesis. The comparison between control and Dif-MSCs groups revealed only a marginal trend (p = 0.075), while no significant difference was found between MSCs and Dif-MSCs (p = 0.329). For osteocytes, ANOVA confirmed significant overall variability among the groups (p = 0.014). These patterns demonstrate a differential impact: undifferentiated MSCs predominantly increase osteoblast proliferation, whereas differentiated MSCs promote maturation into osteocytes, consistent with early-stage cells driving tissue formation and mature cells supporting matrix maintenance. This underscores the importance of differentiation stage when optimizing therapeutic strategies.

For osteocytes, the pattern was inverted: numbers decreased in the MSCs group and increased in the Dif-MSCs group compared with the control, with a statistically significant difference between MSCs and Dif-MSCs (p = 0.006). These findings are consistent with known MSC differentiation mechanisms, whereby undifferentiated cells primarily stimulate osteoblast proliferation and new bone formation, while differentiated cells promote maturation into osteocytes responsible for matrix maintenance. Comparisons of control vs MSCs (p = 0.190) and control vs Dif-MSCs (p = 0.428) did not reach statistical significance. The newly formed bone showed clear organization into compact bone with primary osteons (Haversian systems) (Fig. 5e-f). Hematoxylin-eosin staining appeared more homogeneous with uniform pink coloration, while Van Gieson staining revealed a pinkish-red hue. Together with fewer resorption channels than in the other groups, these features indicate maturity of the bone regenerate.

Cellular composition. In the Dif-MSCs group, osteoblasts were distributed along the surfaces of newly formed bone trabeculae, appearing hyperchromatic with moderate cytoplasm. The mean count of osteoblasts was 40.2 ± 10.5 per 10 HPF. Osteocytes were present in large numbers, embedded within the bone matrix and regularly arranged in lacunae resembling mature lamellar bone, with a mean count of 68.7 ± 14.3 per 10 HPF. Osteoblasts are present along the surfaces of newly formed bone trabeculae; they are hyperchromatic and exhibit a moderate amount of cytoplasm. Osteocytes are observed in large numbers, embedded within the bone matrix and regularly arranged in lacunae resembling those of mature lamellar bone (Fig. 5d-e). Osteoclasts are present but in small numbers, located on remodeling surfaces (reversal lines).

Radiographic assessment confirmed fracture consolidation and gap closure in both experimental groups, with significant improvements in Bridged Cortices, Bridging Callus, and Distal Gap scores from week 4 to 6. The Dif-MSCs group showed superior bridged cortical layers and callus coverage (17.9% and 18.7% greater at week 4; 9.4% and 10.0% greater at week 6) and lower persistent distal gap incidence (−15.6% at week 4, −31.0% at week 6). At week 4, Dif-MSCs exhibited accelerated remodeling with significant CTI reductions (Distal: 4.1%, Proximal: 6.5%, Average: 6.2%), attributed to soft callus formation, endochondral ossification, and osteoclast activation causing transient cortical thinning. This was offset by increased bone density at week 6. Contrasting CTI profiles suggest selective proximal density enhancement, likely due to uneven cell distribution or biomechanical loading “Fig. 6, Table 2”.

Thus, after 1.5 months, a clear gradation of reparative regeneration was observed: Control < MSCs < Dif-MSCs. This was reflected in both the quantity and maturity of the newly formed bone tissue. Fibrous tissue predominated in the control group, whereas bone tissue prevailed in the MSCs and Dif-MSCs groups, with Dif-MSCs providing more rapid formation of mature lamellar bone. Both treatments significantly improved the prognosis for complete closure of the critical defect, with the effect of Dif-MSCs potentially being more pronounced due to the direct supply of osteoblastic cells.

Discussion

The choice of fully differentiated Dif-MSCs (4-week induction) rather than pre-differentiated cells was motivated by evidence that complete ex vivo commitment enhances direct matrix deposition and reduces *in vivo* variability, whereas partial differentiation relies more on paracrine effects and risks incomplete maturation. Our in vitro validation data support this, showing robust ALP upregulation and mineralization absent in undifferentiated MSCs, and align with studies demonstrating superior performance of fully differentiated ADSCs over pre-differentiated cells in critical defect models [9].

The observed hierarchy of regenerative outcomes (Control < MSCs < Dif-MSCs) prompts a detailed examination of the pathophysiological and pathomorphological features of bone repair dynamics in nonunion and delayed fracture consolidation. Undifferentiated MSCs primarily act through paracrine signaling by attenuating local inflammation and recruiting host precursor cells, thereby initiating a fibrocartilaginous bridge. However, owing to their plasticity, these cells may adopt suboptimal fate decisions under mechanical loading or hypoxic conditions, resulting in stable but immature intermediate structures [12]. In contrast, Dif-MSCs streamline this process by directly promoting osteoprogenitor pools, favoring intramembranous pathways and rapid matrix maturation. This is reflected in the accelerated formation of organized lamellar structures and hematopoietic bone marrow. Such differences raise questions about the role of epigenetic priming during ex vivo differentiation, which may increase resistance to fibrotic drift while enhancing autocrine signaling that supports vascular integration and remodeling. This concept is supported by animal studies showing that prior osteogenic priming consistently yields greater microscopic tissue maturity. For example, in a canine radial fracture model, osteogenically differentiated MSC layers reduced external callus formation and inflammation within eight weeks and proved more effective than undifferentiated layers, which predominantly led to fibrous tissue. This suggests that priming mitigates inflammatory barriers and promotes direct bone formation under stable fixation [14].

However, in nonunion cases, mechanical stress and hypoxia may render undifferentiated MSCs more adaptive for initiating repair, albeit with an increased risk of immature structural outcomes. Similarly, in a rabbit bone defect model using xenogeneic grafts enriched with differentiated human bone marrow-derived MSCs, fracture healing was more effective than with undifferentiated counterparts. Radiographic and histopathological evidence demonstrated denser bone formation and accelerated union, attributed to the targeted delivery of committed cells that bypass inductive delays [17]. These parallels underscore a potentially species-independent advantage, although variability in defect size and fixation methods may modulate outcomes. In the present study, unstable fixation combined with a large defect that markedly delays bridging likely amplifies the need for pre-differentiated cells to overcome the progenitor cell deficit. In contrast, for smaller defects or close apposition between fracture fragments, undifferentiated MSCs alone may be sufficient [16]. These data contrast with *in vitro-in vivo* comparisons in which osteogenic differentiation of human MSCs demonstrates enhanced mineralization and matrix organization *ex vivo*, whereas discrepancies arise *in vivo* due to microenvironmental factors such as shear stress or cytokine gradients, which can revert or redirect cellular phenotypes [19]. These observations suggest that mesenchymal stem cells are heterogeneous: their functional behavior strongly depends on tissue of origin, passage number, and donor-specific characteristics. This heterogeneity substantially impacts their practical performance. For instance, undifferentiated adipose-derived cells are relatively inefficient at bone formation and often require additional biological enhancers, whereas bone marrow-derived MSCs respond more consistently to standard differentiation protocols [20]. The inverted pattern – higher osteoblast counts in the MSCs group (52.0 ± 16.2) versus Dif-MSCs (40.2 ± 10.5), and conversely for osteocytes (45.3 ± 5.62 vs. 68.7 ± 14.3) – reflects distinct regeneration dynamics. Undifferentiated MSCs primarily stimulate osteoblast proliferation via paracrine factors such as bone morphogenetic protein-2 (BMP-2) and insulin-like growth factor-1 (IGF-1), thereby promoting early endochondral ossification. By contrast, Dif-MSCs, already committed to the osteogenic lineage, accelerate osteoblast-to-osteocyte transition through enhanced RUNX2-mediated matrix maturation, resulting in reduced proliferation yet increased tissue maturity. These observations align with prior literature [21], which indicates that differentiation diminishes proliferative potential while enhancing osteogenic efficiency *in vivo* models. However, persistent challenges, including issues of cell specificity and immune interactions, may underlie sporadic limitations in therapeutic efficacy, indicating the need for integrating scaffolds to support and stabilize these signaling cues [22].

Van Gieson staining was used in this study for its exceptional sensitivity to extracellular-matrix structural changes, enabling precise evaluation of collagen maturation, callus-formation dynamics, and the degree of tissue consolidation during fracture repair. Primary (woven) bone tissue forms rapidly in early healing and features a chaotic collagen-fiber arrangement, yielding lower density than mature bone. Conversely, secondary (lamellar) bone arises through remodeling with organized parallel fiber alignment. Histologically, immature trabeculae stain purple or pink with yellowish hues, as acid fuchsin penetrates their loose, sparsely packed collagen structure. Mature trabeculae, however, acquire intense bright-red coloration from greater fuchsin retention in tightly packed type I collagen fibers, displacing picric acid (Pathology Outlines, 2023). Van Gieson staining revealed distinct collagen maturation patterns across the groups. The control group exhibited disorganized type I collagen indicative of incomplete remodeling, whereas both MSC-treated groups demonstrated markedly superior matrix

organization. The purplish-red hue in the Dif-MSCs group suggests a transient cartilaginous phase with increased type II/III collagen and proteoglycans, consistent with an endochondral ossification pathway that may accelerate early regeneration yet potentially delay complete mineralization [24]. This observation aligns with literature indicating that differentiated MSCs can promote a more physiological endochondral route akin to natural fracture healing [24], although an excessive cartilaginous phase carries the risk of incomplete remodeling and requires continued monitoring [25]. These findings corroborate data on MSC-based grafts in critical defects, where Van Gieson staining confirmed an organized red matrix in newly formed tissue [23]. Overall, MSCs – particularly their differentiated derivatives – enhance not only the quantity but also the qualitative architecture of regenerating bone tissue, underscoring their role in qualitative restoration of tissue structure rather than mere defect filling. These results offer significant clinical implications for fracture management and its complications; however, therapy optimisation requires careful consideration of divergent osteogenic pathways.

Radiographic findings corroborated the histological observations: the Dif-MSCs group exhibited mature lamellar bone with organised osteons and reduced cartilaginous remnants, aligning with enhanced cortical bridging and callus coverage indicative of accelerated structural union. Transient CTI reductions at week 4—linked to soft callus formation and osteoclast activation—paralleled the histological evidence of early remodelling in Dif-MSCs, including resorption canals and elevated osteocyte counts, suggesting a more efficient transition to secondary osteogenesis compared to undifferentiated MSCs. These outcomes echo Park et al. (2024), who reported comparable integration of morphological and instrumental assessments in rat femoral defect models, where embryonic stem cell-derived MSCs promoted faster bone maturation than controls, as evidenced by micro-CT-derived bone fractional area and density profiles alongside histological matrix organisation [26].

Study Limitations

While this study provides valuable insights into the histopathological effects of MSCs and Dif-MSCs on bone repair, it has notable limitations. The small sample size (n=5 per group) was selected to comply with ethical standards minimizing animal use; however, it may have reduced statistical power, particularly for detecting subtle differences in quantitative parameters such as osteoblast and osteocyte counts. This likely accounts for certain observed trends failing to reach statistical significance (e.g., ANOVA p=0.092 for osteoblasts). Future studies with larger cohorts are recommended to validate these findings and enhance generalizability.

Conclusions

Histological observations indicate that administration of undifferentiated mesenchymal stem cells may enhance the cellular component, including chondrocytes and osteoblasts, within the callus zone, potentially facilitating a more efficient transition from cartilaginous callus to bone tissue via endochondral ossification.

In the group treated with differentiated mesenchymal stem cells, bone formation appears to involve a mixed pattern of intramembranous and endochondral ossification, with limited residual cartilaginous foci. By 6 weeks post-intervention, the newly formed bone tissue demonstrates signs of maturity and advanced regeneration, characterized by lamellar structures that partially bridge the defect, alongside organized bone marrow elements and reduced fibrous or cartilaginous remnants. These preliminary findings suggest differential regenerative potentials, warranting further validation with larger cohorts and additional markers of differentiation efficacy to substantiate the observed trends.

Statement of Ethics: This study protocol was reviewed and approved by the local bioethics committee of Zaporizhzhia State Medical and Pharmaceutical University (protocol No. 12 dated 10.12.2025).

Conflict of Interest Statement: The authors have no conflicts of interest to declare.

Funding Sources: This study was not supported by any sponsor or funder.

Authorship and Contributorship: Maslennikov S., Danukalo M., Isachenko M., Avramenko Yu., Holovakha M., Kolesnyk Yu.: conceptualization, validation, writing - review and editing; Maslennikov S., Danukalo M., Isachenko M., Avramenko Yu.: data curation, formal analysis, investigation, methodology, validation, writing - original draft, and writing - review and editing.

Data Availability Statements. All data generated or analyzed during this study are included in this article. Further enquiries can be directed to the corresponding author.

References

1. Gómez-Barrena E, Padilla-Eguiluz NG, García-Rey E, Hernández-Esteban P, Cordero-Ampuero J, Rubio-Suárez JC, et al. Validation of a long bone fracture non-union healing score after treatment with mesenchymal stromal cells combined to biomaterials. Injury. 2020;51 Suppl 1:S55–S62.
2. Saul D, Menger MM, Ehnert S, Nüssler AK, Histing T, Laschke MW. Bone Healing Gone Wrong: Pathological Fracture Healing and Non-Unions—Overview of Basic and Clinical Aspects and Systematic Review of Risk Factors. Bioengineering (Basel). 2023;10(1):85.
3. Lawry LL, Mani V, Hamm TE, Janvrin M, Juman L, Korona-Bailey J, et al. Qualitative assessment of combat-related injury patterns and injury prevention in Ukraine since the Russian invasion. BMJ Mil Health. doi: 10.1136/military-2024-002863.
4. Tanner MC, Hagelskamp S, Vlachopoulos W, Miska M, Findeisen S, Grimm A, et al. Non-Union Treatment Based on the “Diamond Concept” Is a Clinically Effective and Safe Treatment Option in Older Adults. Clin Interv Aging. 2020;15:1221–1230.
5. Margiana R, Markov A, Zekiy AO, Hamza MU, Al-Dabbagh KA, Al-Zubaidi SH, et al. Clinical application of mesenchymal stem cell in regenerative medicine: a narrative review. Stem Cell Res Ther. 2022;13(1):366.
6. Ferroni L, De Francesco F, Pinton P, Gardin C, Zavan B. Methods to isolate adipose tissue-derived stem cells. Methods Cell Biol. 2022;171:215–228.
7. Hemati S, Ghiasi M, Salimi A. Osteogenic Differentiation of Adipose Tissue-Derived Mesenchymal Stem Cells on Composite Polymeric Scaffolds: A Review. Curr Stem Cell Res Ther. 2025;20(1):33–49.
8. Dadras M, May C, Wagner JM, Wallner C, Becerikli M, Dittfeld S, et al. Comparative proteomic analysis of osteogenic differentiated human adipose tissue and bone marrow-derived stromal cells. J Cell Mol Med. 2020;24(20):11814–11827.
9. Brennan MA, Renaud A, Guilloton F, Mebarki M, Trichet V, Sensebé L, et al. Inferior In Vivo Osteogenesis and Superior Angiogenesis of Human Adipose-Derived Stem Cells Compared with Bone Marrow-Derived Stem Cells Cultured in Xeno-Free Conditions. Stem Cells Translational Medicine, 2017; 6(12), 2160-2172.

10. Mohamed-Ahmed S, Yassin MA, Rashad A, Espedal H, Idris SB, Finne-Wistrand A, et al. Comparison of bone regenerative capacity of donor-matched human adipose-derived and bone marrow mesenchymal stem cells. Cell Tissue Res. 2021 Mar;383(3):1061-1075.

11. Guda T, Stukel Shah JM, Lundquist BD, Macaitis JM, Pérez ML, Pfau-Cloud MR, et al. An In Vivo Assessment of Different Mesenchymal Stromal Cell Tissue Types and Their Differentiation State on a Shape Memory Polymer Scaffold for Bone Regeneration. J Biomed Mater Res B Appl Biomater. 2024 Dec;112(12):e35516.

12. Mollentze J, Durandt C, Pepper MS. An In Vitro and In Vivo Comparison of Osteogenic Differentiation of Human Mesenchymal Stromal/Stem Cells. Stem Cells Int. 2021 Sep 8;2021:9919361.

13. Yoon Y, Khan IU, Choi KU, Jung T, Jo K, Lee SH, et al. Different Bone Healing Effects of Undifferentiated and Osteogenic Differentiated Mesenchymal Stromal Cell Sheets in Canine Radial Fracture Model. Tissue Eng Regen Med. 2017 Nov 15;15(1):115-124.

14. Peer BA, Bhat AR, Shabir U, Bharti MK, Bhat IA, Pandey S, et al. Comparative evaluation of fracture healing potential of differentiated and undifferentiated guinea pig and canine bone marrow-derived mesenchymal stem cells in a guinea pig model. Tissue Cell. 2022;76:101768.

15. Yi N, Zeng Q, Zheng C, Li S, Lv B, Wang C, et al. Functional variation among mesenchymal stem cells derived from different tissue sources. PeerJ. 2024 Jun 28;12:e17616.

16. Han X, Liao R, Li X, Zhang C, Huo S, Qin L, et al. Mesenchymal stem cells in treating human diseases: molecular mechanisms and clinical studies. Sig Transduct Target Ther. 2025;10:262.

17. van Boxtel J, Uguten M, Harmsen MC, Stevens HP, van Dongen JA. Isolation of Stromal Vascular Fraction by Fractionation of Adipose Tissue. Methods Mol Biol. 2025;2922:97–111.

18. Tong L, Yang Z, Dai W, Sun Z, Yang J, Xue Q, et al. Experimental study on determining the degree of bone healing by wall thickness ratio analysis. J Orthop Surg Res. 2024;19(1):79.

19. Cho S, Choi H, Jeong H, Kwon SY, Roh EJ, Jeong KH, et al. Preclinical Study of Human Bone Marrow-Derived Mesenchymal Stem Cells Using a 3-Dimensional Manufacturing Setting for Enhancing Spinal Fusion. Stem Cells Transl Med. 2022;11(10):1072-1088.

20. Zhang Z, Yang X, Cao X, Qin A, Zhao J. Current applications of adipose-derived mesenchymal stem cells in bone repair and regeneration: A review of cell experiments, animal models, and clinical trials. Front Bioeng Biotechnol. 2022;10:942128.

21. Zhu S, Chen W, Masson A. Cell signaling and transcriptional regulation of osteoblast lineage commitment, differentiation, bone formation, and homeostasis. Cell Discov. 2024;10:71.

22. Stamnitz S, Klimczak A. Mesenchymal Stem Cells, Bioactive Factors, and Scaffolds in Bone Repair: From Research Perspectives to Clinical Practice. Cells. 2021;10(8):1925.

23. Shi W, Gao Y, Wu Y, Tang Y, Bian L, Que Y, et al. Human nasal mucosa ectomesenchymal stem cells derived extracellular vesicles loaded omentum/chitosan composite scaffolds enhance skull defects regeneration. Int J Biol Macromol. 2023;248:125924.

24. Yang X, Zhang S, Lu J, Chen X, Zheng T, He R, et al. Therapeutic potential of mesenchymal stem cell-derived exosomes in skeletal diseases. Front Mol Biosci. 2024 Jun 6;11:1268019.

25. Baek D, Park KH, Lee KM, Jung S, Joung S, Kim J, et al. Ubiquitin-specific protease 53 promotes osteogenic differentiation of human bone marrow-derived mesenchymal stem cells. Cell Death Dis. 2021;12:238.

26. Park JH, Bae HS, Kim I, Jung J, Roh Y, Lee D, et al. Efficacy of Bone Regeneration Cell Therapy Using Mesenchymal Stem Cells Originating from Embryonic Stem Cells in Animal Models; Bone Defects and Osteomyelitis. Tissue Eng Regen Med. 2025 Jan;22(1):145-157.

Figure legends

Figure 1. Determination of the decalcification endpoint (from 1st day till 15th).

Figure 2. Calcium deposition in mesenchymal stem cells demonstrated by Alizarin Red staining on day 30 of culture. (a) Undifferentiated control MSCs. (b) Osteogenically differentiated MSCs. Original magnification ×40 (ZEISS Primo Vert microscope).

Figure 3. Histological staining of bone specimens from rabbits in the control group. (a) Fibrous tissue with newly formed bony spicules and trabeculae within the defect zone in the control group. H&E stain, Mag.×50; (b) Defect area with well-developed anastomosing bony trabeculae. Van Gieson stain, Mag.×200; (c) Newly formed bone tissue, immature and heterogeneous in cellular distribution, with small residual foci of cartilaginous tissue. H&E stain, Mag.×200; (d) Fibrous tissue showing focal edema, mild lymphocytic–macrophage inflammatory infiltration, and an increased number of small blood vessels. Van Gieson stain, Mag.×200.

Figure 4. Histological staining of bone sections from rabbits in Group 2 (MSCs). (a) Cartilaginous callus with newly formed bone tissue in the bone regenerate zone of the MSC-treated group. H&E stain, Mag.×50; (b) Calcified, anastomosing cartilaginous trabeculae with deposited bone tissue in the bone regenerate zone of the MSCs-treated group. H&E stain, Mag.×400; (c) Cartilaginous callus with heterogeneous staining: eosinophilic bone tissue and mineralized cartilaginous trabeculae in the bone regenerate zone of the MSCs-group. H&E stain, Mag.×200; (d) Presence of yellow and red bone marrow in the central regions of the bone regenerate zone of the MSCs-group. H&E stain, Mag.×200; (e) Newly formed bone tissue structurally resembling normal cancellous and cortical bone, with a large number of resorption canals in the bone regenerate zone of the MSCs-group. H&E stain, Mag.×400; (f) Hypertrophic chondrocytes with degenerative changes in areas of calcified cartilage in the bone regenerate zone of the MSCs-group. H&E stain, Mag.×400.

Figure 5. Histological staining of bone sections from rabbits in Group 3 (Dif-MSCs). (a) Compact bone tissue in the bone regenerate zone of the Dif-MSCs group. H&E stain, Mag.×400; (b) Compact bone tissue in the bone regenerate zone with mature tri-lineage red bone marrow in the central region of the regenerate in the Dif-MSCs group. Van Gieson stain, Mag.×200; (c) Cancellous bone tissue in the bone regenerate zone with residual fibrous tissue at the margins of the defect and active regeneration in the Dif-MSCs group. H&E stain, Mag.×200; (d) Cancellous bone tissue in the bone regenerate zone with periosteal cells along the outer bone surface. Osteocytes embedded in the lamellar bone matrix and empty lacunae containing apoptotic osteocytes in the Dif-MSCs group. Van Gieson stain, Mag.×400; (e) Compact bone tissue in the bone regenerate zone showing signs of organization, including the formation of primary osteons and lamellae of the bone matrix in the Dif-MSCs group. Van Gieson stain, Mag.×400; (f) Cancellous bone tissue in the bone regenerate zone with a resorption canal in which bone tissue has been removed and replaced by newly formed tissue in the form of osteons in the Dif-MSCs group. Van Gieson stain, Mag.×400.

Figure 6. Representative radiographs of the operated hind limbs in experimental rabbits Dif-MSCs group: (a) 4 weeks after cell transplantation (b) 6 weeks after cell transplantation.

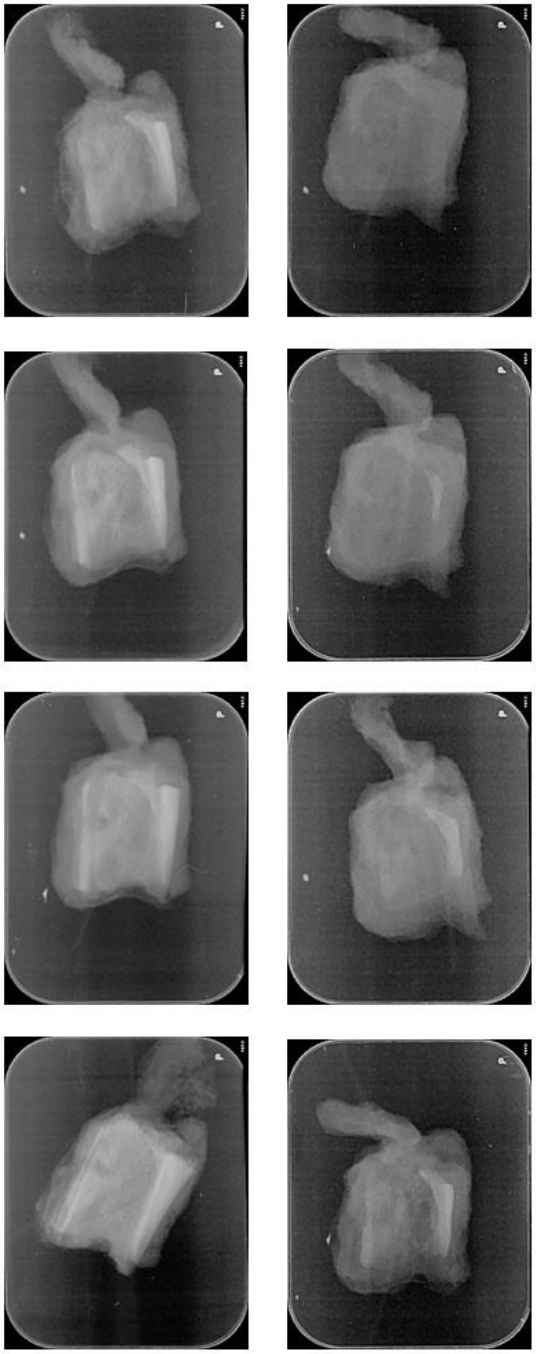

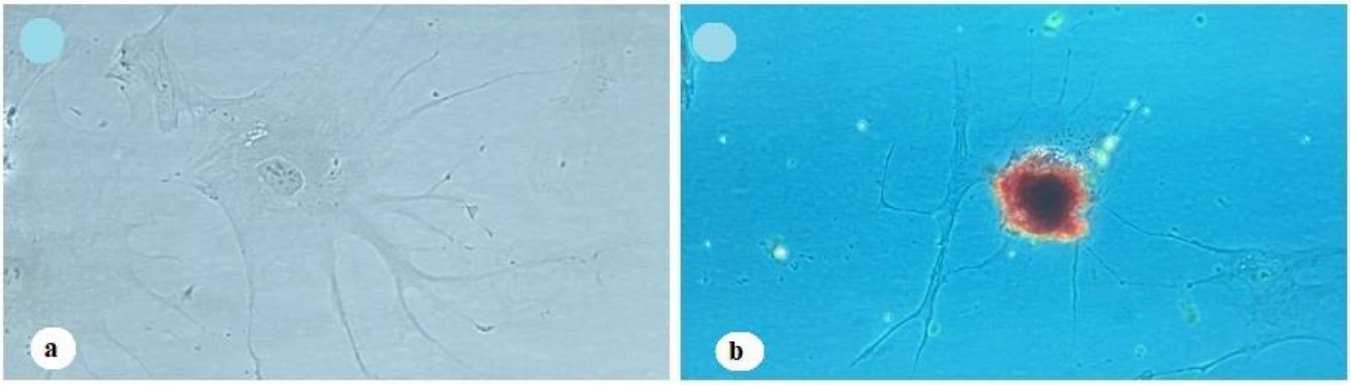

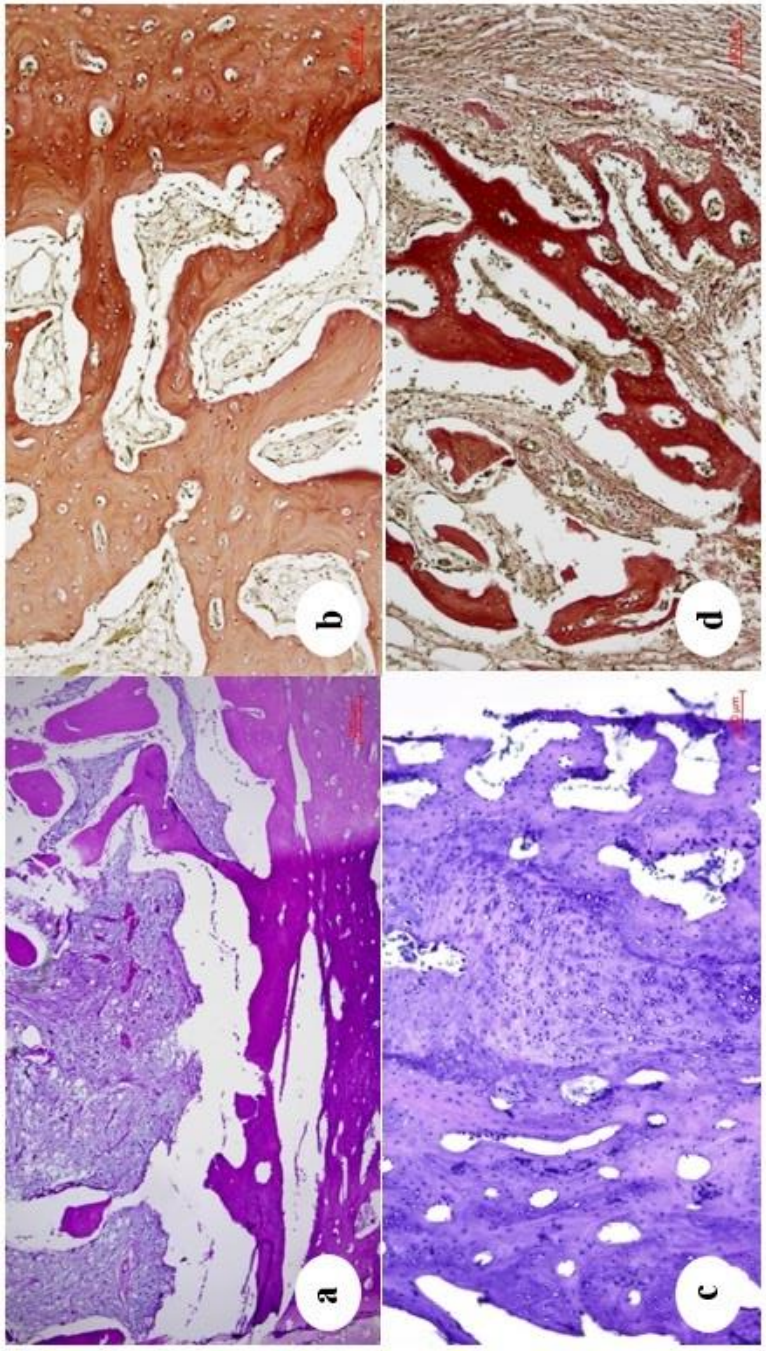

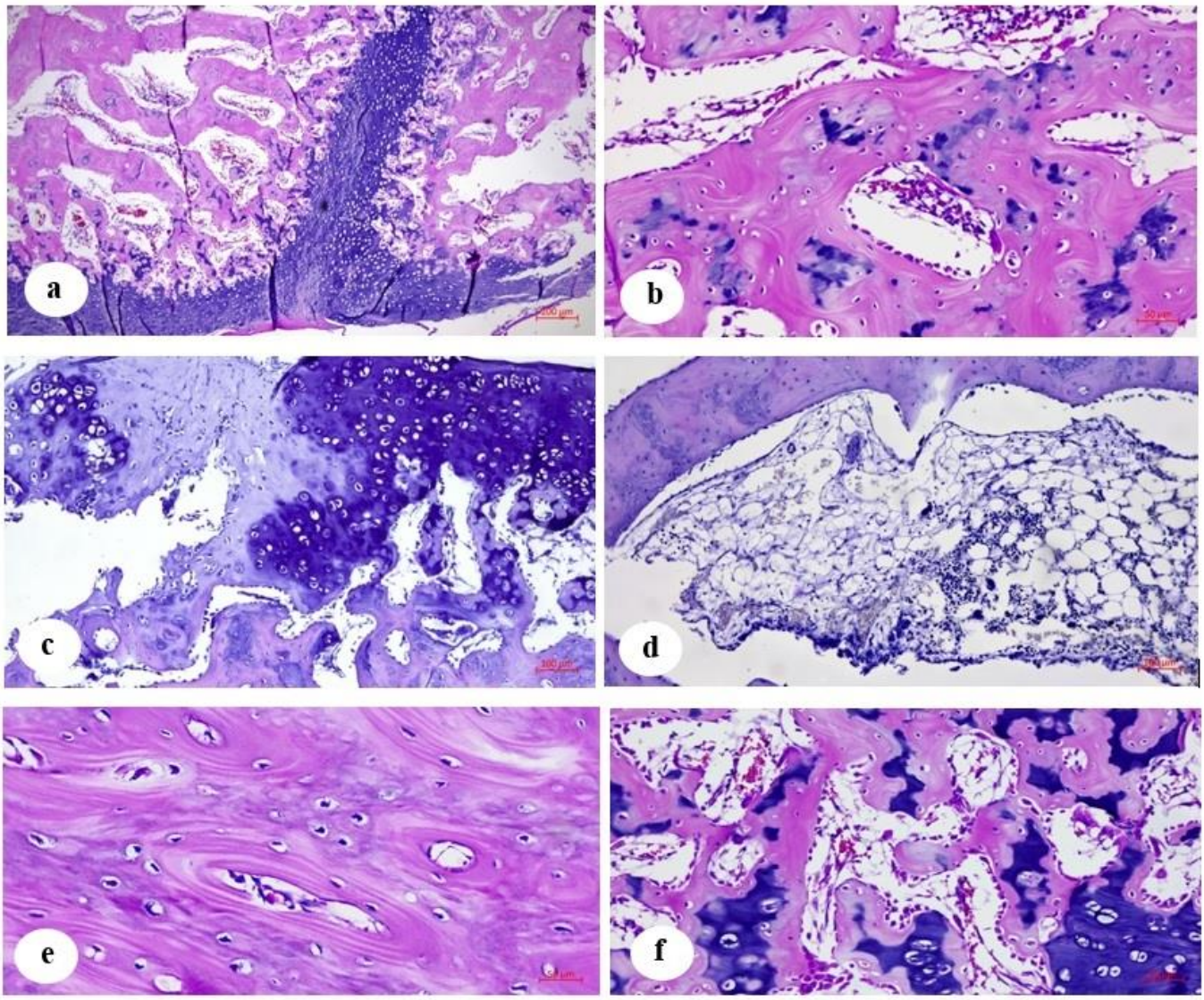

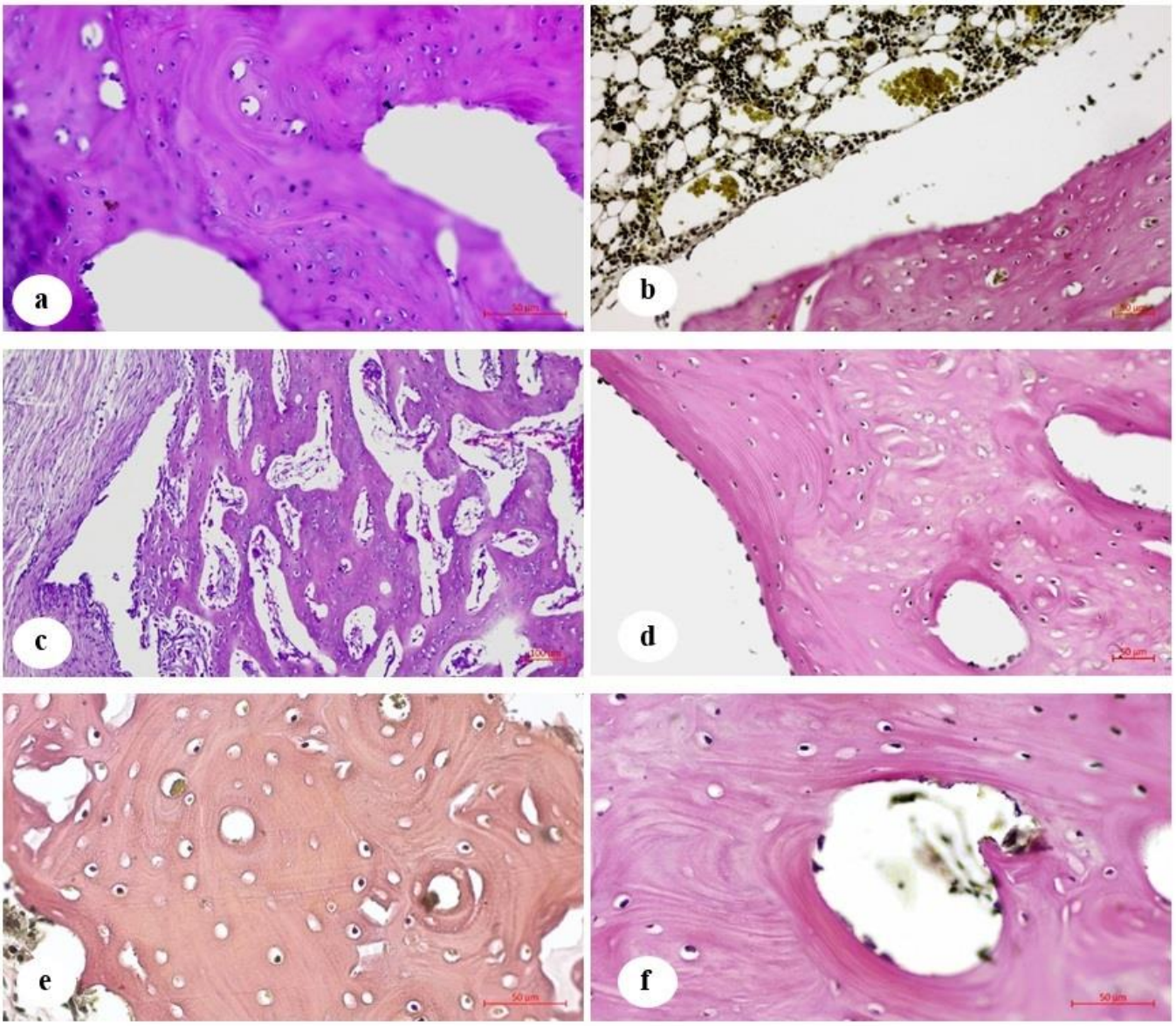

Table 1. Quantitative ratio of osteoblasts/osteocytes in the fracture regeneration zone following the application of different cellular agents (mean ± SD, 10 HPF).

	Group	mean ± SD	ANOVA F (*p* value)	Comparison with Control Group (Welch's *t*-test *p*)	Comparison with MSCs Group (Welch's *t*-test *p*)
Osteoblasts	**Control Group**	28.6 ± 7.0	F=3.064 (0.092)	-	-
	MSCs	52.0 ± 16.2		0.032*	-
	Dif-MSCs	42.7 ± 11.5		0.075	0.329
Osteocytes	**Control Group**	58.4 ± 12.0	F=6.662 (0.014*)	-	-
	MSCs	45.3 ± 5.62		0.190	-
	Dif-MSCs	65.7 ± 9.76		0.428	0.006*

*****Statistically significant difference at $p < 0.05$.

Table 2. Radiographic parameters in the groups at 4 and 6 weeks after cell transplantation into the fracture site. Data are presented as median (Q1; Q3).

Indicators	MSCs		Dif-MSCs		*p*-values were calculated using two-tailed paired Student's t-tests.
	4 weeks	6 weeks	4 weeks.	6 weeks	
Bridged Cortices, %	2.29 (2.23;2.31)	3.20 (3.14;3.21)	2.70 (2.65;2.70)	3.50 (3.45;3.50)	*p**=0.0001 *p***=0.0001 *p*#=0.0001 *p*##=0.0001
Bridging Callus, %	57.30 (55.80;57.70)	80.00 (78.50;80.20)	68.00 (67.80;68.20)	88.00 (87.80;88.00)	*p**=0.0001 *p***=0.0001 *p*#=0.0001 *p*##=0.0001
Distal Gap, %	39.10 (39.10;43.20)	17.40 (16.20;17.80)	33.00 (32.50;33.80)	12.00 (12.00;12.50)	*p**=0.0001 *p***=0.0001 *p*#=0.0001 *p*##=0.0001
CTI Distal (Cortical thickness index)	0.49 (0.49;0.50)	0.49 (0.47;0.49)	0.47 (0.46;0.47)	0.48 (0.47;0.48)	*p**=0.1328 *p***=0.0955 *p*#=0.0068 *p*##=0.5346
CTI Proximal	0.46 (0.45;0.46)	0.44 (0.44;0.44)	0.43 (0.42;0.43)	0.44 (0.43;0.44)	*p**=0.1434 *p***=0.0955 *p*#=0.0085 *p*##=0.3734
CTI Average	0.48 (0.47;0.48)	0.46 (0.45;0.46)	0.45 (0.44;0.45)	0.46 (0.45;0.46)	*p**=0.0216 *p***=0.0955 *p*#=0.0022 *p*##=1.0000

Note. Statistical significance: p - MSCs group, 4 weeks vs 6 weeks; p** - Dif-MSCs, 4 weeks vs 6 weeks; p# - MSCs group vs Dif-MSCs group at 4 weeks; p## - MSCs group vs Dif-MSCs group at 6 weeks.*